ISIJ International, Vol. 30 (1990), No. 10, pp. 802-811

Review

Creep Deformation of Engineering Alloys: Developments from Physical Modelling

B.F. DYSON and M. McLEAN[1)]

Division of Materials Metrology, National Physical Laboratory, Teddington, Middlesex, TW11 0LW, U.K.
Now at Department of Materials, Imperial College, London, SW7 2BP, U.K.

1) National Physical Laboratory.

(*Received on March 2, 1990; accepted in the final form on April 20, 1990*)

Differences in the creep behaviour of particle-strengthened engineering alloys relative to simple solid solutions are reviewed and their implications for the mechanisms of high temperature deformation in these materials are considered. Constitutive equations describing the shapes of creep curves, based on physical models of the important types of damage are considered. These are incorporated in a computer software package, designated CRISPEN, that allows the analysis of creep data, the development of a detabase of model parameters and the simulation of the strain/time trajectory for arbitrary loading conditions. Examples of the application of CRISPEN to a range of alloys and loading conditions are described.

KEY WORDS: creep; fracture; deformation; modelling; constitutive equations; damage; mechanisms; computer analysis.

1. Introduction

Advances in design procedures for high temperature plant, involving sophisticated computer analyses, are making new demands on the data required to describe the material performance. Whereas the older methods of design-to-code could operate on abbreviated measures of material performance (*e.g.*, rupture life, minimum creep rate, time to an arbitrary strain), the new approaches which attempt to simulate the service behaviour of components can only be effectively implemented if there is an adequate representation of the full strain–time evolution of the material under the appropriate applied stress/temperature history.

There have been many attempts to model the creep behaviour of metals to account for various aspects of the shapes of creep curves and these have met with varying degrees of success. It is tempting to search for a universal description that will apply to all, or at least to most, high temperature materials. However, as will be discussed in the following section, there are very important differences in the high temperature mechanical behaviour of various classes of materials that clearly imply the operation of specific mechanisms and the appropriateness of different mathematical representations of the data. It is important, therefore, to have a formalism that is capable of accommodating these variants in physical mechanisms for different materials and for different loading conditions. This is of particular importance when it is intended to extrapolate from a limited database to conditions for which data are not available, either to different constant stress/temperature regimes or to variable or complex loading conditions and environments.

There have been two general approaches to representing the evolution of creep strain, ε. The most common and apparently most direct is to describe strain simply as functions of stress, temperature and time (*e.g.*, Evans *et al.*[1)]).

$$\varepsilon = \varepsilon(\sigma, T, t) \quad \text{.....(1)}$$

This can provide an accurate empirical description of constant stress or constant load creep curves; however, if calculations involving changing stresses and temperatures are required then arbitrary rules defining transitions between different creep curves must be developed. Alternatively, the creep behaviour can be represented by a series of coupled rate equations which describe the rate of evolution of strain and of the relevant state variables S_1, S_2, . . . that control the rate of deformation.[2)]

$$\left.\begin{aligned} \dot{\varepsilon} &= f(\sigma, T, S_1, S_2, \ldots) \\ \dot{S}_1 &= g(\sigma, T, S_1, S_2, \ldots) \\ \dot{S}_2 &= h(\sigma, T, S_1, S_2, \ldots) \end{aligned}\right\} \quad \text{.....(2)}$$

If the explicit forms of Eq. Set (2) are known, then the creep curve can be determined by numerical integration; moreover, the procedures can easily cope with complex stress/temperature histories.

In many engineering alloys, including nickel-base superalloys as well as certain creep resistant steels and aluminium alloys, the creep behaviour is dominated by a progressively increasing creep rate that is caused by microstructural changes in the material that may be considered to be "damage". Kachanov[3)] and subsequent workers[4,5)] developed the discipline of Continuum Damage Mechanics to account for this type of behaviour; specific empirical equations were developed, in the form of Eq. Set (2), to account

for the observed creep behaviour. More recently Ashby and Dyson[6] have considered the implications of detailed damage micro-mechanisms for the precise forms of Eq. Set (2); this was described as physics inspired empiricism. Some of these have now been implemented into a software package, designated CRISPEN, that operates on IBM compatible personal computers to allow (i) the analysis of creep data, (ii) the development of an appropriate database, and (iii) the simulation of creep deformation for arbitrary (including varying) loading conditions.[7,8]

This paper will review the development of the models incorporated in CRISPEN, describe the approaches to the data analysis and give examples of its application to a range of materials.

2. Comparison of the Creep Behaviour of Solid Solution and Particle Strengthened Alloys

The traditional approaches to representing creep data have evolved from extensive and detailed studies of relatively simple materials such as pure metals and single phase alloys. In particular, the identification of a steady state creep rate which can be represented as a power law function of stress and with a temperature dependence similar to that of the self diffusion coefficient has a clear mechanistic basis for these simple materials.[9] However, although the procedures continue to be used to provide an empirical mapping of data for more complex alloys, there is no theoretical validity for doing so. Here we consider the important differences between the creep behaviour of simple and complex engineering alloys that must be taken into account when modelling creep deformation in these materials.

2.1. *Shapes of Creep Curves*

Fig. 1 illustrates the essential differences in the shapes of creep curves found in solid solution and particle-hardened alloys. In pure metals and simple alloys, there is generally a relatively short initial period of decreasing creep rate (primary) that is associated with hardening of the material due to the accumulation of dislocations and a final short period of sharply increasing creep rate (tertiary) that results from the initiation and growth of damage such as cavities and cracks; most of the creep life is dominated by a constant, or steady state, creep rate that is thought to be associated with a stable dislocation substructure. However, in many complex engineering alloys, apparently steady state behaviour is now believed to reflect the inaccuracy of the measurement technique rather than an intrinsic material property: after a short primary regime, there is a progressively increasing creep rate that is caused by the development of ' damage ' processes other than cavitation, except when the ductility, ϵ_f, is low (1–2 %). Dyson and McLean[10] showed that there was an empirical correlation in nickel-base superalloys of high ductility between the increasing creep rate and accumulated creep strain, and that the creep rate was not strongly dependent on the (changing) particle size. Indeed

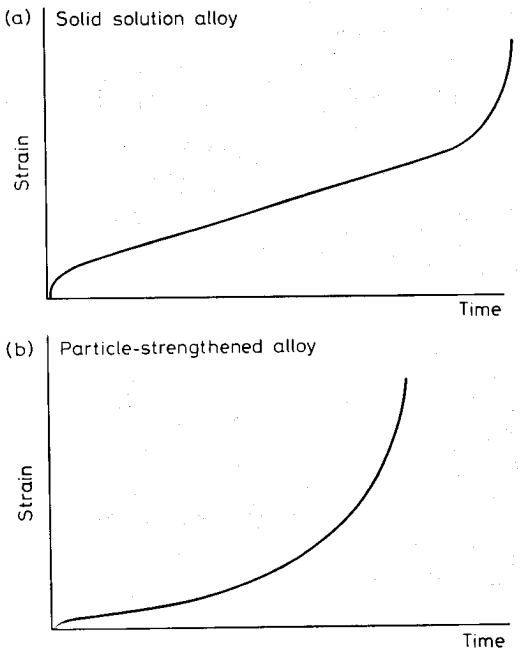

Fig. 1. Schematic illustration of the shapes of creep curves.

there are indications that the increasing creep rate is accompanied by an increase in dislocation density rather than by the development of a steady-state substructure.[11]

2.2. *Creep Rate Equations*

In pure metals and other simple solid solution alloys, the dominant steady-state creep rate $\dot{\varepsilon}_{ss}$ is commonly represented as a function of stress and temperature by the following power law and exponential functions.

$$\dot{\varepsilon}_{ss} = \dot{\varepsilon}_0 \left[\frac{\sigma}{\sigma_0}\right]^n \exp\left[-\frac{Q}{RT}\right] \quad \text{.....(3)}$$

For these materials, the observed values of $n \sim 4$ and $Q \sim$ activation energy for self diffusion are quite consistent with models which regard the steady state as being a dynamic balance between hardening and recovery.[12,13] Use of Eq. (3) to describe creep rate data for complex alloys requires very high values of n and Q and various modifications of Eq. (3) have been proposed to accommodate the results for such complex alloys.[14,15] However, there are indications that these data may be better represented by an exponential function of stress; this suggests a radical change in the controlling mechanism from one of recovery-controlled mobile dislocation density to one of diffusion-controlled dislocation motion.

2.3. *Constant Stress vs. Constant Load Tests*

For simple metals and alloys of high ductility, there is a very significant difference between the creep curves produced under constant load and constant stress conditions. This is due to the dominant effect of changing testpiece cross-section in increasing the stress, and therefore the creep rate, to accelerate tertiary creep under constant load conditions. How-

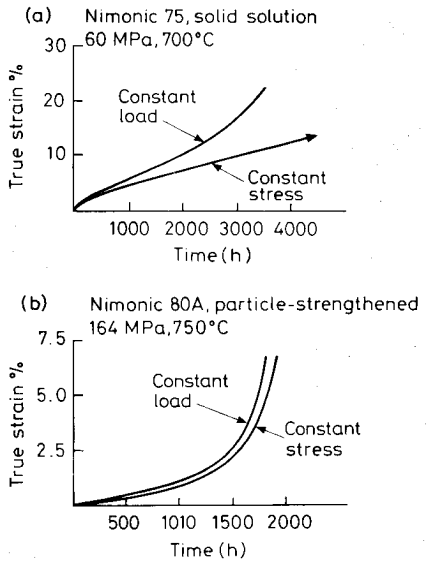

Fig. 2. Comparison of the creep curves for constant-stress and constant-load tensile tests.

ever, for particle-strengthened materials there is relatively little difference between the creep curves produced under conditions of constant load and constant stress.[16] Fig. 2 shows the differences between constant load and constant stress creep curves for solid solution and particle-strengthened alloys. This suggests that the geometrical and cavitation factors which dominate in the simple alloys are minor compared with other causes of tertiary creep in particle-strengthened alloys that are intrinsic to the material microstructure. In the case of superalloys, the observation of tertiary creep in compressive loading[17] clearly eliminates cavitation as the dominant cause.

2.4. *Prestrain*

The application of plastic prestrain prior to creep testing has quite different effects on solid solution and particle-strengthened materials. In the former, increasing plastic prestrain leads to a progressive reduction in creep rates[18] whereas for particle-strengthened materials, there is an increase in creep rate.[19,20] Since creep fracture strain in metallic materials is generally reduced by prior plastic deformation (due to initiation of grain boundary cavities[21]) the conclusion is that it is the increasing mobile dislocation density that leads to a reduction in creep strength of particle-strengthened alloys.[21] This contrasts sharply with the well known conclusion that creep strengths of simple solid solution alloys increase with dislocation density.

3. Physical Modelling of a Creep Curve

3.1. *Individual Damage Categories*

The following discussion will concentrate on reviewing the models that account for the increasing creep rate (*i.e.*, tertiary creep) that dominates the high temperature deformation of many particle-strengthened alloys. Ashby and Dyson[6] identified three categories of damage that could contribute to tertiary creep:

(i) loss of external section due to geometrical changes during creep;
(ii) loss of internal load-bearing section due to the development of cavitation; and
(iii) changes in the material microstructure, such as the density of dislocations and the size of particles.

Categories (i) and (ii) will be generally common to both simple and complex alloys.

(i) Loss of External Section

For a power-law creeping material under conditions of constant load, L, the stress σ at any instant is determined by the cross-sectional area, A, and:

$$\sigma = \frac{L}{A}$$

Assuming constant volume, V, of a cylindrical specimen of gauge length, l, then:

$$dV = Adl + ldA = 0$$

Thus

$$\frac{dA}{A} = -\frac{dl}{l} = -d\varepsilon$$

and therefore:

$$A = A_i e^{-\varepsilon} \quad \text{or} \quad \sigma = \sigma_i e^{\varepsilon}$$

The consequences of such loss of external section on $\dot{\varepsilon}$ can be represented by a set of equations of the form of Eq. (2) by defining an appropriate state variable ω_1. However, there is no unique way of doing so; the physical effect of loss of load bearing area can be represented by different mathematical formulations which lead to equation sets which appear to be quite different, but which can be integrated to give precisely the same result.

In the present work, the various forms of damage have been defined so that they increase linearly with strain. For the case of loss of external section, damage is defined as $\omega_1 = n \ln (A_i/A) = n\varepsilon$:

$$\left.\begin{aligned} \dot{\varepsilon} &= \dot{\varepsilon}_i e^{\omega_1} \\ \dot{\omega}_i &= n\dot{\varepsilon} \end{aligned}\right\} \quad \text{.....(4)}$$

Here the state variable ω_1 can take any value from 0 to ∞ (*i.e.*, ω is unbounded).

It is conventional in Continuum Damage Mechanics (CDM) to define a damage parameter, w_1 that falls within the range 0 to 1. Taking $w_1 = (1 - A/A_i) \equiv (1 - \sigma_i/\sigma)$ leads to the following coupled rate equations:

$$\left.\begin{aligned} \dot{\varepsilon} &= \dot{\varepsilon}_i \left[\frac{1}{1-w_1}\right]^n \\ \dot{w}_1 &= \dot{\varepsilon}_i \left[\frac{1}{1-w_1}\right]^{n-1} \end{aligned}\right\} \quad \text{.....(5)}$$

$\dot{\varepsilon}_i$ is the initial creep rate in the absence of any primary. Eq. Set (4) or (5) can be used to generate the trajectory of strain as a function of time for any arbitrary history of load and temperature: under the

conditions of constant load and temperature used to generate creep data, they both reduce to:

$$\dot{\varepsilon} = \dot{\varepsilon}_i \exp(n\varepsilon) \quad \text{.....(6)}$$

and

$$\therefore \quad \varepsilon = \frac{1}{n} \ln [1 - n\dot{\varepsilon}_i t]^{-1} \quad \text{.....(7)}$$

These alternative formulations of damage are related by the transformation

$$w_1 \rightarrow 1 - e^{-\omega_1/n}.$$

(ii) Loss of Internal Section

Dyson and Gibbons[22] have treated the case of loss of internal section due to continuous nucleation and subsequent growth of cavities at a rate constrained by the surrounding sound material. The rate of change of creep rate in the tertiary stage is sensitive to the magnitude of the fracture strain, ε_f, which itself is an indicator of the propensity of the alloy to develop such damage. They show that an approximate CDM description of this phenomenon can be written in the following form:

$$\left.\begin{aligned} \dot{\varepsilon} &= \dot{\varepsilon}_i e^{\omega_2} \\ \dot{\omega}_2 &= \frac{n}{3\varepsilon_f}\dot{\varepsilon} \end{aligned}\right\} \quad \text{.....(8)}$$

The damage parameter, ω_2, represents the area fraction occupied by creep-constrained grain boundaries with zero load-carrying capacity. Under conditions of constant stress and temperature, Eq. Set (8) reduces to:

$$\dot{\varepsilon} = \dot{\varepsilon}_i \exp(n/3\varepsilon_f)\varepsilon \quad \text{.....(9)}$$

and

$$\therefore \quad \varepsilon = \frac{3\varepsilon_f}{n} \ln\left[1 - \frac{n}{3\varepsilon_f}\dot{\varepsilon}_i t\right]^{-1} \quad \text{.....(10)}$$

As in the previous case, an alternative damage w_2 can be defined to have values $0 \leqslant w_2 \leqslant 1$ but which integrates to exactly the same strain trajectory.

(iii) Change in the Material Microstructure

The major difference between the two general types of alloy (simple solid solution and particle-hardened) appears to be in relation to the role of changing dislocation density in modifying the creep rate, rather than to effects caused by ageing of particles.[10] Here we consider the simplest of models in order to identify the important influences.

The strain rate $\dot{\varepsilon}$ can be expressed in terms of the density of *mobile* dislocations ρ_m and their mean velocity v by the Orowan equation:

$$\dot{\varepsilon} = \rho_m b v \quad \text{.....(11)}$$

The rate of change of creep rate that characterises the shape of a creep curve in the absence of any other type of damage is determined by the evolution rates of ρ_m and v (b is the Burger's vector which is a constant). Similarly, the effect of prior plastic deformation on $\dot{\varepsilon}$ will depend on the changes in ρ_m and v induced by plastic deformation. A universal creep equation derived from dislocation dynamics is not available, but the essential differences in creep behaviour between simple alloys and complex high temperature engineering alloys highlighted in the preceeding section can be explained in the following manner.

The mobile dislocation density can be expressed in terms of the total dislocation density, ρ, by $\rho_m = \psi\rho$, where ψ, which varies from 0 to 1, depends on many (unquantifiable) factors *viz.*:

- The uniformity of the individual dislocation link lengths; the more single functioned the distribution, the larger ψ is likely to be, particularly when the mean stress due to the dislocation network approaches σ.
- The geometrical arrangement of the dislocations; for example a large fraction contained in subboundaries will reduce ψ.
- The mechanism of dislocation motion; for example, ψ will approach zero when dislocation motion is fast, which is the case in athermal glide.

With our present state of knowledge, neither the initial magnitude of ψ nor its rate of evolution can be calculated. Nevertheless, a simple deterministic model of creep can be developed by assuming that the dislocation link lengths are uniformly sized and remain so as ρ increases. Thus:

$$\left.\begin{aligned} \dot{\varepsilon} &= \psi_i \rho b v \\ d\psi/d\rho &= 0 \end{aligned}\right\} \quad \text{.....(12)}$$

where ψ_i is a characteristic of the material.

The evolution of ρ with time is given by:

$$\dot{\rho} = \delta' v\rho - R'\rho^2 \quad \text{.....(13)}$$

The first term on the right is a dislocation multiplication term (Alexander and Haasen[23]); δ' is called the dislocation breeding coefficient. The second term on the right takes account of the reduction in dislocation density by recovery and was first suggested by Friedel[24]; R' contains the kinetic terms. There are two extremes in the creep behaviour represented by Eqs. (12) and (13):

(1) At small values of ρ (early stages of creep) and/or R (low temperatures) the second term on the right hand side of Eq. (13) can be neglected and Eqs. (11) and (13) can be rearranged to give sets of equations of the form of Eq. (2). Taking $\omega_3 = (\rho - \rho_i)/\rho_i$, where ρ_i is the initial dislocation density and ω_3 is therefore unbounded, the following simple equation set is obtained.

$$\left.\begin{aligned} \dot{\varepsilon} &= \dot{\varepsilon}_i(1+\omega_3) \\ \dot{\omega}_3 &= C\dot{\varepsilon} \end{aligned}\right\} \quad \text{.....(14)}$$

Again the damage ω_3 increases linearly with strain; $\dot{\varepsilon}_i = \psi_i \rho_i b v_i$ is the initial creep rate in the absence of any primary creep, $v = v_i$ (constant) and $C = \delta'/\psi_i b \rho_i$.

Alternatively, by defining $w_3 = (1 - \rho_i/\rho) = \omega_3/(1+\omega_3)$, we can express the same creep behaviour with the advantage, for some purposes, that $0 \leqslant w_3 \leqslant 1$.

$$\left.\begin{aligned} \dot{\varepsilon} &= \dot{\varepsilon}_i(1-w_3)^{-1} \\ \dot{w}_3 &= C\dot{\varepsilon}_i(1-w_3) \end{aligned}\right\} \quad \text{.....(15)}$$

Under conditions of constant stress and tempera-

ture Eq. Sets (14) and (15) become:

$$\dot{\varepsilon} = \dot{\varepsilon}_i(1+C\varepsilon) \equiv \dot{\varepsilon}_i \exp\left[\frac{t}{\tau_1}\right] \quad \text{.....(16)}$$

and $$\therefore \quad \varepsilon = \frac{1}{C}[\exp(C\dot{\varepsilon}_i t) - 1] \quad \text{.....(17)}$$

where, $\tau_1 = 1/\delta' v \equiv 1/C\dot{\varepsilon}_i$: the time constant characterising the increase in creep rate.

An important point to note is that $\dot{\varepsilon}_i$ and τ_1 are, respectively, proportional and inversely proportional to v and so strain rates and the shapes of creep curves are both sensitive to v.

A further point is that the creep rate at constant stress and temperature increases linearly with strain, in contrast to the two previous damage mechanisms which result in an exponential increase in strain rate. We call these two types of tertiary damage linear strain softening (Eq. (16)) and exponential strain softening (Eqs. (6) and (9)), respectively. Eq. (16) predicts a monotonically increasing creep rate until some other damage mechanism (fracture or mechanical instability) intervenes; this is because a constant dislocation velocity has been assumed. When creep occurs by thermally activated glide (as it does in Class I solid solution alloys[9]) or by climb/glide (as it does in particle-hardened alloys below the yield stress) then $v = v(\sigma - \alpha\mu b\sqrt{\rho})$ and strain rate will therefore decrease as strain accumulates to give rise to a sigmoidal shape of creep curve.[25] Again, fracture or instability mechanisms may intervene before a sigmoidal shape is observed. Dyson and McLean[10] were the first to recognise that Eq. (16) represented the creep behaviour of nickel-base alloys and proposed the dislocation mechanism. The prediction that $C \propto 1/\rho_i$ has recently been demonstrated[26] and the mechanism clearly explains the observation that creep rates increase with prior plastic deformation. More recent confirmation that the velocity of dislocations can limit creep (by climb/glide) in nickel-base superalloys has been obtained by the observation of sigmoidal creep at very low stresses, Fig. 3[27]; a quantitative explanation has been given using the above arguments and a sinh function for the velocity.[25,26]

In the case of dislocation yield by glide, ψ will decrease as the stress approaches $\alpha\mu b\sqrt{\rho}$, and this may also contribute to climb controlled dislocation motion; however, this is not considered further here.

(2) The second term in Eq. (13) becomes increasingly important as ρ and/or R increases; in particular, when ρ is sufficiently high that the decrease in v with increasing ρ is dominant then $\delta' v$ becomes a hardening coefficient. A steady-state is reached when $\dot{\rho} = 0$ giving, from Eq. (13):

$$\rho_{ss} = \frac{\delta' v}{R'} \quad \text{.....(18)}$$

In pure metals and Class II solid solution alloys, dislocations move at approximately the speed of sound and so v can be regarded as a constant and $\rho_{ss} \simeq (\sigma/\alpha\mu b)^2$. Thus Eq. (16) can be rearranged to give:

$$\dot{\varepsilon}_{ss} = \frac{\psi_i R'}{\delta' b^3 \alpha^4}\left[\frac{\sigma}{\mu}\right]^4 \quad \text{.....(19)}$$

Thus a pure metal or Class II solid solution alloy is predicted to have a steady state creep rate proportional to σ^4 and independent of v. Furthermore, the activation energy will be contained in the recovery term R' and will thus be the same as that for self diffusion. Prior plastic deformation will result—with this deterministic model—in zero creep (assuming that the yield stress decreases with increasing temperature) until recovery processes fulfil the condition $\sigma > \alpha\mu b\sqrt{\rho}$ after an incubation time that will increase with increasing amounts of prestrain. In reality, finite creep rates will be observed due to the inhomogeneous distribution of dislocation link lengths in real materials: the solution requires a probabilistic approach, such as McLean's,[12] but with a suitable distribution function to describe the link lengths. Since dislocations move at speeds approaching the velocity of sound in pure metals and Class II solid solution alloys, the time constant for the initial transient (given by Eq. (16)) is very low and a 'plastic' strain is usually observed on loading. The simple deterministic model then predicts an immediate steady state creep rate given by Eq. (19): in reality there will be a primary stage, again due to the distribution in dislocation link lengths.

In Class I solid solutions and particle-hardened materials, where the dislocation velocity is a function of ρ, the shape of the inverse transient creep curve and the asymptotic steady-state creep rate depend on the relative magnitudes of the recovery parameter R' and the dislocation generation term $\delta' v$ in Eq. (13).

3.2. *Generalised Equation Set*

In practice the various types of damage can occur simultaneously. Consequently, their effects must be combined in an appropriate way. In the following data analysis, the various factors combine in product form that is consistent with stress redistribution from damaged to sound material. In the analysis, a linear hardening term with associated internal stress S is included to account for primary creep.[7] The combined effects of all of these factors are represented by the following equation set in which all three types of tertiary damage increase linearly with strain and have *unbounded values*.

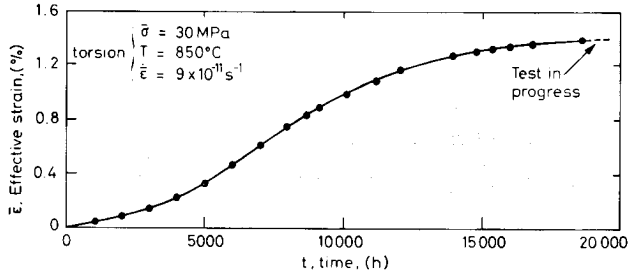

Fig. 3. Creep curve at low stress in torsion for Nimonic 90 showing sigmoidal creep.

$$\left.\begin{aligned}\dot{\varepsilon} &= \dot{\varepsilon}_i(1-S)(1+\omega_3)e^{(\omega_1+\omega_2)}\\ \dot{S} &= H\dot{\varepsilon}_i(1-S)-RS\\ \dot{\omega}_1 &= n\dot{\varepsilon}\\ \dot{\omega}_2 &= \frac{n}{3\varepsilon_f}\dot{\varepsilon}\\ \omega_3 &= C\dot{\varepsilon}\end{aligned}\right\} \quad \text{.....(20)}$$

The additional model parameters for primary creep are a hardening coefficient H and a recovery coefficient R that leads to a steady state value of internal stress.

$$S_{ss} = \left[1+\frac{R}{H\dot{\varepsilon}_i}\right]^{-1}.$$

Not all of the damage mechanisms will occur for every test and every material. Consequently the set of equations must be modified to the circumstances of a particular test. For example, tertiary damage ω_1 accounts for the increasing stress during constant load testing; in constant stress creep tests $\omega_1=0$. Also ω_2 accounts for the development of creep cavitation; this does not occur in compression testing and is not significant in some high ductility materials. Thus, directionally solidified and single crystal superalloys do not fail by creep cavitation, but by the development of geometrical instabilities: in these circumstances, $\omega_2=0$.

(An equally valid set of equations with each " damage " defined to have a maximum value of 1 can be developed.)

4. Data Analysis Procedures

The models described in the previous section and expressed in the general form of Eq. Set (20) have formed the basis of a software package designated CRISPEN to be used for the analysis of creep data for engineering alloys; the development of a database of model parameters; and the simulation of creep deformation under arbitrary loading conditions.

The first problem is to identify a reliable procedure for determining the values of the model parameters required to describe a given set of creep data. During the evolution of the CRISPEN software, three approaches of increasing sophistication have been adopted in determining the model parameters ($\dot{\varepsilon}_i$, H, R, C).

4.1. *Method 1*

It was assumed that one of the damage mechanisms would be so dominant that Eq. Set (20) could be reduced to contain *either* linear *or* exponential expressions for tertiary creep.

$$\left.\begin{aligned}\dot{\varepsilon} &= \dot{\varepsilon}_i(1-S)(1+\omega)\\ \dot{S} &= H\dot{\varepsilon}_i(1-S)-RS\\ \dot{\omega} &= C\dot{\varepsilon}\end{aligned}\right\} \quad \text{.....(21)}$$

or

$$\left.\begin{aligned}\dot{\varepsilon} &= \dot{\varepsilon}_i(1-S)e^{\omega}\\ \dot{S} &= H\dot{\varepsilon}_i(1-S)-RS\\ \dot{\omega} &= C'\dot{\varepsilon}\end{aligned}\right\} \quad \text{.....(22)}$$

A creep curve can be described approximately by four operational parameters, defined in Fig. 4, and there are simple relationships between the set of operational parameters and the model parameters appropriate to either the linear or exponential formulations (Table 1).[7]

However, experience shows that analysis of strain/time creep curves does not give a clear discrimination between the linear and exponential representations of tertiary creep.

4.2. *Method 2*

Differential forms of the creep curves are more sensitive indicators of the appropriate mechanisms and can be analysed in a fairly straight forward manner to give estimates of the model parameters. Again this strategy has, in the first instance, assumed a single dominant type of tertiary creep mechanism leading to Eq. Set (21) or (22).

The primary creep parameters—in both cases (H, R)—can be determined by plotting the data points during primary creep in the form $\dot{\varepsilon}/\dot{\varepsilon}_{\min}$ as a function of primary creep strain as shown in Fig. 5(a). The straight line obtained is consistent with the model proposed; the intercept and gradient of this plot have values $R/(R+H\dot{\varepsilon}_{\min})$ and $(R+H\dot{\varepsilon}_{\min})/\dot{\varepsilon}_{\min}$, respectively, from which H and R can be determined by simple manipulation.

For tertiary creep, analogous differential plots provide an important diagnostic procedure for determining if the data are best described by either the linear or exponential formulations. Thus for the linear formulation, a plot of $\dot{\varepsilon}/\dot{\varepsilon}_{\min}$ as a function of ε in the tertiary regime is a straight line with a gradient C;

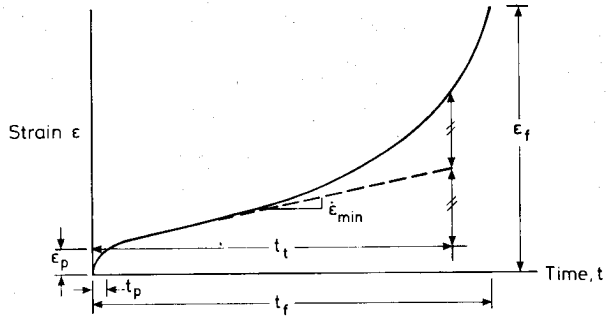

Fig. 4. Schematic creep curve displayed as strain as a function of time showing the definition of operational parameters defining the shape of the creep curve.

Table 1. Relationship between operational parameters describing the shape of a creep curve and the model parameters used in Eqs. (21) and (22).

Model parameter	Operational parameter
$\dot{\varepsilon}_i$	$\dot{\varepsilon}_{\min}$
R	$\dot{\varepsilon}^2_{\min}t_p/\varepsilon_p$
H	$\left\{\varepsilon_p\left[1+\frac{\dot{\varepsilon}_{\min}t_p}{\varepsilon_p}\right]^2\right\}^{-1}$
C	$\ln 3.5/\dot{\varepsilon}_i t_t$
C'	$\ln 4.9/2\dot{\varepsilon}_{\min}t_t$

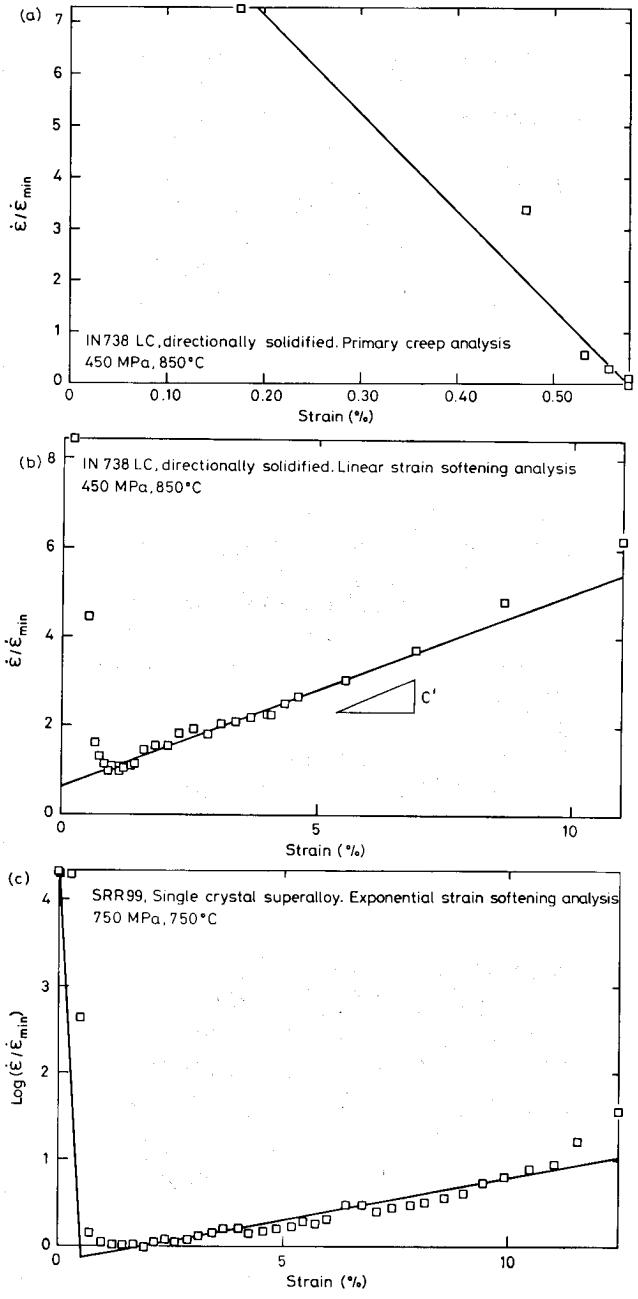

(a) Primary: $(\dot{\varepsilon}/\dot{\varepsilon}_{\min})$ as a function of $\dot{\varepsilon}_p$
(b) Linear strain softening: $(\dot{\varepsilon}/\dot{\varepsilon}_{\min})$ *vs.* ε
(c) Exponential strain softening: $\log(\dot{\varepsilon}/\dot{\varepsilon}_{\min})$ *vs.* ε

Fig. 5. Creep curves displayed as various functional forms of creep rate $\dot{\varepsilon}$ and strain ε to identify the operative models and to evaluate the model parameters.

for the exponential model, $\log(\dot{\varepsilon}/\dot{\varepsilon}_{\min})$ as a function of ε is linear with a slope C'. Examples of data best described by each formulation are shown in Figs. 5(b) and 5(c).

Having established H, R, and C (or C') which characterise the shape of the creep curve, a reference creep rate $\dot{\varepsilon}_{\text{ref}}$, which differs in general from $\dot{\varepsilon}_{\min}$, is determined by a process of successive approximations to give the best fit of the model to the data.

A procedure has been developed to allow different damage mechanisms, which are represented by exponential functions, to be taken into account (Barbosa *et al.*[8]). This recognises that $(1+\omega_3)\sim\exp(\omega_3)$ for a range of values of ω_3. Consequently a composite damage $W=\omega_1+\omega_2+\omega_3$ is defined and Eq. Set (20) approximated in the following way:

$$\left.\begin{aligned}\dot{\varepsilon} &= \dot{\varepsilon}_{\text{ref}}(1-S)\exp W\\ \dot{S} &= H\dot{\varepsilon}_i(1-S)-RS\\ \dot{W} &= C'_{\text{eff}}\dot{\varepsilon}\end{aligned}\right\} \quad \text{.....(23)}$$

The parameter set (H, R, $\dot{\varepsilon}_{\text{ref}}$, C'_{eff}) is determined as described above and then the various contributions to C'_{eff} are partitioned depending on the type of test and material. Examples of the contributions to C'_{eff} are shown in Table 2.

Table 2. Relationship between C'_{eff} (Eq. (23)) and various contributions to tertiary creep in different types of test.

Type of load	Load control	Material behaviour in uniaxial tension	C'_{eff}
Constant load	Tension	Cavitating	$C'+n+\frac{n}{3\varepsilon_f}$
		Necking	$C'+n$
Constant stress	Tension	Cavitating	$C'+\frac{n}{3\varepsilon_f}$
		Necking	C'
Constant load	Compression		$C'-n$
Constant stress	Compression		C'

4.3. *Method 3*

As the survey of the models in Chap. 3 clearly shows, the various factors contributing to tertiary creep lead to a combination of *both* the linear *and* exponential formulations. Method 2 is adequate when one of these models dominates, but breaks down when both are significant. The current CRISPEN analysis addresses this mixed-mode problem by restricting the strain over which the analysis is carried out so that the exponential factor can be approximated to a linear expansion with a small error. An effective linear softening coefficient C_{eff} can be partitioned into various components in exactly the same way as that for the multiple-exponential damage described in Method 2. However in this case, the creep curve is calculated using the full mixed linear/exponential Eq. Set (20).

Examples of this type of fit of the model, as both strain/time and strain rate/strain plots, are shown in Fig. 6.

5. Application of CRISPEN to Analyse Data for Engineering Alloys

The CRISPEN data analysis procedure has been applied to a wide range of engineering materials that depend to various extents on the presence of particles to enhance the creep strength. Typical examples of the agreement between the experimental data and the creep curves predicted by CRISPEN from the analysis of individual creep curves are shown in Fig. 7. The

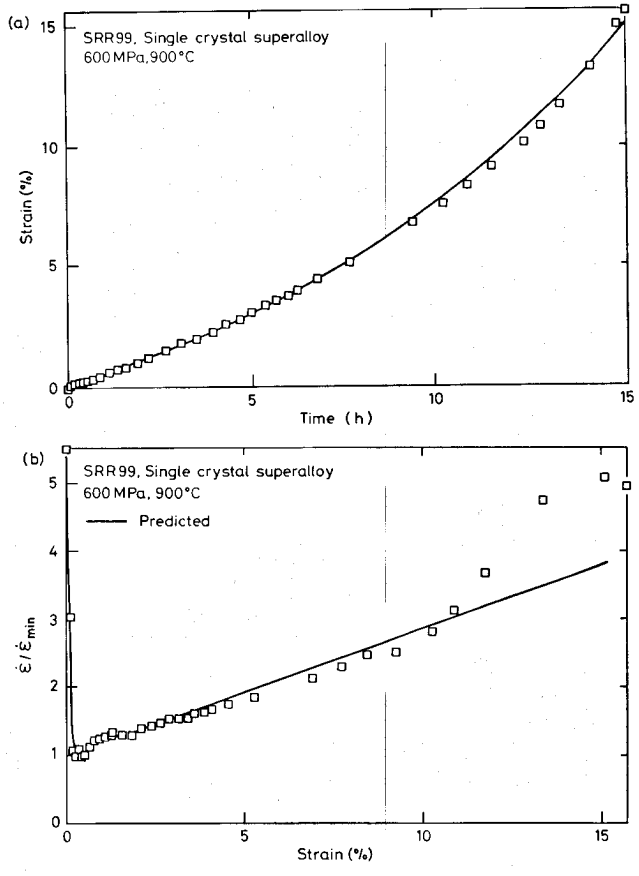

(a) Strain as a function of time
(b) Strain rate as a function of strain

Fig. 6. Example of the agreement between experimental data and the CRISPEN representation based on Eq. (20).

approach appears to represent successfully the creep behaviour of creep resistant steels, nickel-base superalloys and, even, some metal matrix composites.

Having established the combination of model parameters ($\dot{\varepsilon}_{ref}$, H, R, C) together with a knowledge of n and ε_f for each test condition, this information constitutes a database from which predictive calculations can be made for arbitrary test conditions. Examination of the variation of each of these parameters with stress and temperature shows that $\dot{\varepsilon}_{ref}$ is the most sensitive to loading conditions; the other parameters vary much more slowly. Two approaches have been used with CRISPEN to operate on this database to predict the strain/time evolution for arbitrary test conditions.

(1) The variation of $\dot{\varepsilon}_{ref}$ with stress and temperature is examined in terms of a power-law creep equation. Every data point is given values of n and Q to represent the local variation with stress and temperature (n and Q can be quite stress and/or temperature dependent). For an arbitrary loading condition, the database is scanned to identify the closest stress/temperature condition for which data are available and this is used as a reference from which the required condition is simulated. The parameters (H, R, C) for the reference are assumed to apply to the condition of the calculation; however, an appropriate value of $\dot{\varepsilon}_{ref}$ is extrapolated from that of the reference using the values of n and Q. This is similar to assuming that the Monkman–Grant parameter is a constant over the range of test conditions defined by the reference test and the conditions for which calculations are being made.

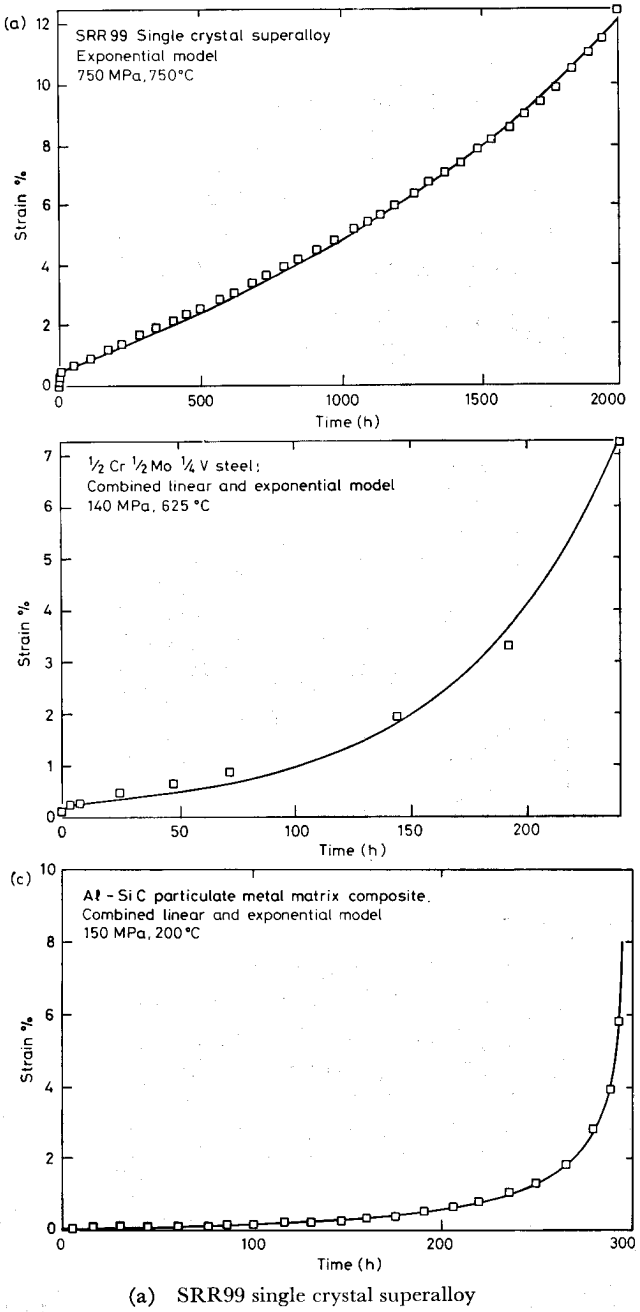

(a) SRR99 single crystal superalloy
(b) CrMoV creep resistant steel
(c) Al–SiC metal matrix composite

Fig. 7. Comparisons of the CRISPEN representation of creep curves for various materials.

(2) In some cases where sufficient data are available, explicit expressions describing the various model parameters as functions of stress and temperature are used in the simulation algorithm.

An example of extrapolation from a short-term reference condition to predict long-term behaviour for the superalloy IN738LC in the directionally solidified form is shown in Fig. 8. In practice it is not recommended that such long extrapolations (from a 400 h

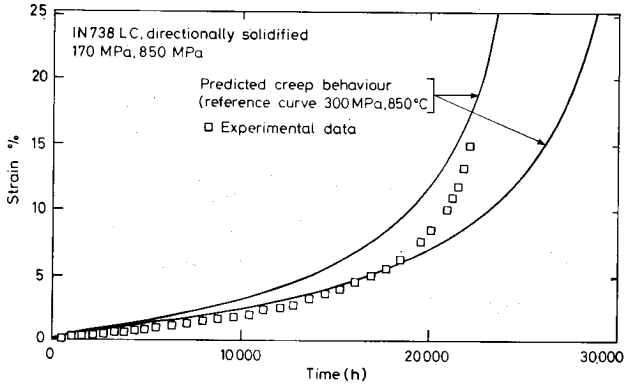

Fig. 8. Comparison of experimental data for a long-term creep test with the curve predicted from a short-term reference curve for IN738LC.

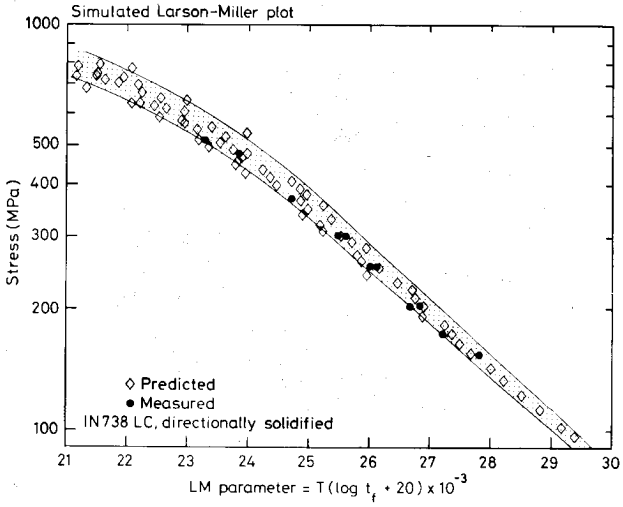

Fig. 9. Larson–Millar plot for IN738LC constructed from creep lives for random stress and temperatures calculated using CRISPEN. Experimental data constituting the CRISPEN database are shown for reference.

test to predict 20 000 h life) be used, however it does indicate a potential for limited extension of a database.

An alternative indicator of the validity of the CRISPEN predictions is shown in the simulated Larson–Miller plot for superalloy IN738LC shown in Fig. 9. This was constructed by randomly selecting stresses and temperatures and allowing CRISPEN to predict the lives. The lives given by the actual data which provided the database from which calculations have been made are shown as solid points; lives calculated using the reference curve approach for a wide range of stresses and temperatures are shown as open triangles. The predicted scatter in the Larson–Miller plot is no greater than that of the real data. This is a useful calibrant of the predictions which gives some confidence in the more detailed predictions that can be given by the analysis.

An extensive database for the single crystal superalloy SRR99 for constant stress creep tests on [100] oriented crystals has been analysed and the various parameters represented as explicit analytical functions of stress and temperature. Fig. 10 shows the close

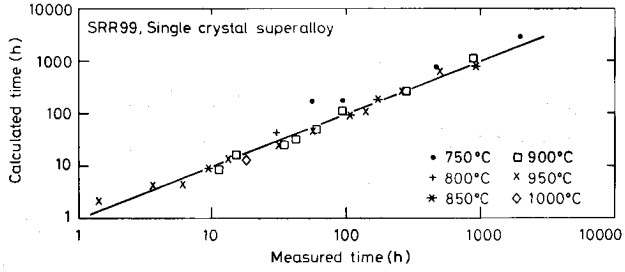

Fig. 10. Comparison of measured and calculated creep rupture lives for all test conditions available for SRR99, a single crystal superalloy.

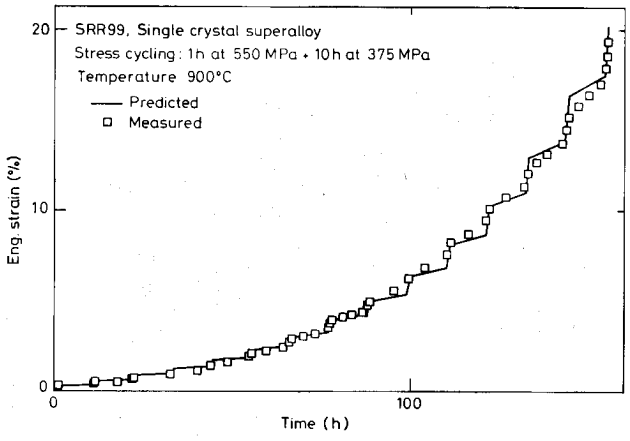

Fig. 11. Comparison of the measured creep curve for cyclic stressing of SRR99 with the calculated curve based on a constant stress database.

agreement between the measured fracture lives for each test and the values calculated by CRISPEN from the functional representations of the various model parameters.

As discussed earlier, the effects of varying stress and temperature are automatically taken into account in the calculations. Fig. 11 shows the predicted strain/time plot for a cyclic creep test on SRR99, calculated from a constant stress database; the experimental data are shown for reference.

6. Discussion and Forward Look

In developing the CRISPEN software, constitutive equations based on current understanding of the physics of deformation and fracture have been used to represent experimental creep data. Simple procedures have been developed to analyse the data and to calculate the creep deformation for arbitrary loading conditions. This has been successfully applied to a number of engineering alloys both to describe individual creep curves and to make limited extrapolations. However, if the sole intention is to model the shapes of creep curves, the technique has no substantial advantage over empirical curve-fitting methods (such as the θ-projection[1]). The important benefits of a state-variable approach, such as that used in developing CRISPEN, over a description of strain as a function of loading history derive from the flexibility of the approach in allowing (a) variable and more

complex loading conditions to be addressed and (b) extension of the calculations to incorporate other factors.

Ghosh *et al.*[28] have recently described an extension of the CRISPEN analysis to account for the variation of creep behaviour with crystallographic orientation for a nickel-base superalloy. This involved reformulation of the various equations in terms of shear rather than tensile stresses and strain and the restriction of deformation to specific slip systems that are observed to be active. This follows the underlying philosophy of the CRISPEN development of being guided by current knowledge of the physics controlling the process.

In another study, Dyson and Osgerby[29] have considered the effects of simultaneous oxidation and creep deformation, and have extended the coupled differential equation sets to account for synergy between these phenomena. It has been particularly successful in predicting the effect of testpiece size on creep behaviour.

Acknowledgements

This paper reviews work to which several colleagues at the National Physical Laboratory and Cambridge University have made significant contributions. The data on the single crystal superalloy SRR99 were provided by Dr. M. Winstone of the Royal Aerospace Establishment.

REFERENCES

1) R. W. Evans, J. D. Parker and B. Wilshire: Recent Advances in Creep and Fracture of Engineering Materials and Structures, ed. by B. Wilshire and D.R.J. Owen, Pineridge Press, Swansea, (1982), 235.
2) H. J. Frost and M. F. Ashby: Deformation-Mechanism Maps, Pergamon Press, Oxford, (1982).
3) L. M. Kachanov: *IZV. Akad. Nauk SSSR*, (1958), No. 8, 26.
4) Yu. N. Rabotnov: Proc. of XII IUTAM Congress, Stanford, ed. by H. Hetenyi and W. G. Vincenti, Springer-Verlag, Berlin, (1969), 32.
5) F. A. Leckie and D. R. Hayhurst: *Acta metall.*, **25** (1977), 1059.
6) M. F. Ashby and B. F. Dyson: Proc. of 6th Int. Conf. on Fracture (ICF6), New Delhi, ed. by D. Taplin, Pergamon Press, Oxford, (1984), 3.
7) J. C. Ion, A. Barbosa, M. F. Ashby, B. F. Dyson and M. McLean: NPL Report DMA A115, National Physical Laboratory, April 1986.
8) A. Barbosa, N. G. Taylor, M. F. Ashby, B. F. Dyson and M. McLean: Proc. of 6th Int. Symp. on Superalloys, ed. by D. Duhl *et al.*, Metall. Soc. of AIME, New York, (1988), 683.
9) O. D. Sherby and P. M. Burke: *Prog. Mater. Sci.*, **13** (1968), 325.
10) B. F. Dyson and M. McLean: *Acta metall.*, **31** (1983), 1203.
11) P. J. Henderson and M. McLean: *Acta metall.*, **31** (1983), 1203.
12) D. McLean: *Rep. Prog. Phys.*, **29** (1966), 1.
13) R. Lagneberg: *J. Mater. Sci.*, **3** (1968), 596.
14) P. L. Threadgill and B. Wilshire: Proc. Conf. on Creep Strength of Steels, Met. Soc., London, (1974), 8.
15) B. Reppich: Proc. of 12th Vortragsveranstaltung VDEh, FVW, in press.
16) M. S. Loveday and B. F. Dyson: Proc. of 4th Int. Conf. on "Creep and Fracture of Engineering Materials and Structures", Inst. Met., London, (1990), 941.
17) G. P. Tilly and G. F. Harrison: *J. Strain Analysis*, **8** (1973), 124.
18) P. W. Davies, J. D. Richards and B. Wilshire: *J. Inst. Met.*, **90** (1961–62), 431.
19) R. N. Wilson: *Royal Aircraft Est. Tech. Rep.*, **69132**, (1969).
20) J. A. Williams and T. C. Lindley: *Z. Metalkd.*, **60** (1969), 957.
21) B. F. Dyson and M. J. Rodgers: *Met. Sci.*, **8** (1974), 261.
22) B. F. Dyson and T. B. Gibbons: *Acta metall.*, **35** (1987), 2355.
23) H. Alexander and P. Haasen: *Solid State Phys.*, **22** (1968), 27.
24) J. Friedel: Dislocations, Pergamon Press, Oxford, (1964).
25) B. F. Dyson: *Rev. Phys. Appl.*, **23** (1988), 605.
26) B. F. Dyson: Modelling of Mateiral Behaviour and Design, ed. by J. D. Embury and A. W. Thompson, Miner., Met. and Mater. Soc., Warrendale, MA, (1990), 59.
27) R. Timmins: "The Creep and Fracture of a Nickel-Base Superalloy under Uniaxial and Shear Stresses", PhD Thesis, University of Sheffield, (1988).
28) R. N. Ghosh, R. V. Curtis and M. McLean: *Acta metall.*, (1990), in press.
29) B. F. Dyson and S. Osgerby: Materials and Engineering Design: The Next Decade, ed. by B. F. Dyson and D. R. Hayhurst, Inst. Met., London, (1989), 373.